

# A Comparative Study of Electromagnetic Fields Excited by Vertical Dipole on the Earth

Priyaranjan

*Research Scholar, Dept. of Physics, J.P. University, chapra*

---

## ARTICLE DETAILS

### Article History

Published Online: 30 December 2017

### Keywords

Electromagnetic, Dipole, Earth

---

## ABSTRACT

*In this paper, a comparative study of electromagnetic fields excited by vertical electric Dipole on the earth is presented for the both planar and spherical earth models. The exact field expression in the spherical earth model is considered as an accurate solution and reference to the planar earth model. Numerical results show that the residue series gives a good approximation to the field.*

---

## 1. INTRODUCTION

The fields are expressed by spherical harmonics series which is usually poor in convergence although the solution is exact. In order to overcome the poor convergence problem, several research works have focused on the accelerated summation of the spherical harmonics. Johler [1] and Lewis [2] calculated the fields at an extremely low frequency (ELF) directly from zonal harmonics series, using the Kummer's transformation with an averaging process for a sharply bounded ionosphere model. Johler further improved the convergence of the harmonics series by using the modified zonal harmonics and geometric series [3].

In addition to the zonal harmonics series solutions, several asymptotic methods were also explored using the Watson's transformation. Sommerfeld [4] derived the field expressions for a perfectly conducting earth. Wait [5] and Fock [6] derived the formulas of the fields radiated by a dipole in the presence of a homogeneous earth with a compact notation for the Hankel function of the order one-third. The boundary conditions at the surface of the sphere were specified by a surface impedance. The asymptotic formulas for the electromagnetic field over the spherical conductor covered with a dielectric layer are derived in [7]. The trapped surface wave was extracted out and it also proved that the trapped surface wave can be efficiently excited when the thickness of the dielectric layer is larger than a certain value. The fields expressions are further extended for the spherical earth coated with an  $n$ -layered dielectric in [8].

Both of the planar and spherical earth models can be simplified under certain approximations, for instance the residue series approach. Therefore, their accuracy and validation range need to be studied in detail. In addition, it is not difficult to find that there exist in literature a number of results of radiated electric and magnetic fields derived for the planar stratified media, they are, however, not straightforwardly verified or validated for the accuracy. Due to this reason, some interests have been shown along the first line. It was indicated that to obtain the closed form solutions or the fast convergent solution, some conditions must be applied [9]–[16], as very well summarized by Collin [17], [18]. In fact, some other research works were also done earlier to look into the lateral wave properties [19]–[24]. The properties of total field presented in [19]–[24] are shown to fluctuating in near zone versus the horizontal distance while the asymptomatic forms given in [25], [26], [27]–[29], [9], [10] cannot predict such effects.

In this paper, the accelerated spherical harmonics series in the spherical model by full-wave method is compared with the residue series. The accuracy of the residue series is confirmed for the perfect conducting sphere. For the layered sphere, the results show that the hybrid effect due to the trapped surface wave and the lateral wave was ignored in the residue series; and according to the full-wave method, the hybrid effect becomes stronger with the increase of the permittivity of the dielectric layer.

## 2. FORMULATION :

The field generated by a vertical electric dipole in the air with a unit electric dipole moment in the three-layered medium was given in [26], where a time dependence of  $e^{-i\omega t}$  was assumed and it is used subsequently but will be suppressed. The height of the dipole is while the height of the observation point is  $z_r$ , both measured from the surface of the dielectric layer. The medium consists of a half-space of air (region 0,  $z \leq 0$ ), a dielectric layer with thickness (region 1,  $0 \leq z \leq 1$ ), and a conducting or dielectric medium (region 2,  $1 \leq z$ ). The height of the dipole is from the surface of the dielectric layer. The wave numbers of the three regions are denoted by  $k_0$ ,  $\omega \sqrt{\epsilon_0 \mu_0}$ ,  $k_1 = \sqrt{\epsilon_{r1}} k_0$ , and  $k_2 = \sqrt{\epsilon_{r2} + i\sigma / \omega \epsilon_0} k_0$ , respectively.

The total electric field is expressed as a sum of the direct wave  $E_z^{(1)}$ , the reflected wave  $E_z^{(2)}$ , and the contributions from the lateral and surface waves  $E_z^{(3)}$  as follows:

$$E_z^{(1)} = \frac{\omega\mu_0}{4\pi k_0} e^{ik_0 r_1} \left[ \frac{ik_0}{r_1} - \frac{1}{r_1^2} - \frac{i}{k_0 r_1^3} - \left( \frac{z_r - z_s}{r_1} \right)^2 \cdot \left( \frac{ik_0}{r_1} - \frac{3}{r_1^2} - \frac{3i}{k_0 r_1^3} \right) \right] \tag{1a}$$

$$E_z^{(2)} = \frac{\omega\mu_0}{4\pi k_0} e^{ik_0 r_2} \left[ \frac{ik_0}{r_2} - \frac{1}{r_2^2} - \frac{i}{k_0 r_2^3} - \left( \frac{z_r + z_s}{r_2} \right)^2 \cdot \left( \frac{ik_0}{r_2} - \frac{3}{r_2^2} - \frac{3i}{k_0 r_2^3} \right) \right] \tag{1b}$$

$$E_z^{(3)} = -\frac{\omega\mu_0}{4\pi k_0^2} \cdot \int_{-\infty}^{\infty} \frac{A(\lambda) H_0^{(1)}(\lambda\rho) \cdot e^{i\gamma_0(z_r+z_s)} \lambda^3}{q(\lambda)\gamma_0} d\lambda \tag{1c}$$

where

$$q(\lambda) = \frac{\gamma_0}{k_0^2} + \frac{\gamma_2}{k_2^2} - i \left( \frac{\gamma_0 \gamma_2 k_1^2}{k_0^2 k_2^2 \gamma_1} + \frac{\gamma_1}{k_1^2} \right) \tan(\gamma_1 l) \tag{2a}$$

$$A(\lambda) = -\frac{\gamma_2}{k_2^2} + i \frac{\gamma_1}{k_1^2} \tan(\gamma_1 l) \tag{2b}$$

$$r_1 = \sqrt{\rho^2 + (z_r - z_s)^2} \tag{2c}$$

$$r_2 = \sqrt{\rho^2 + (z_r + z_s)^2} \tag{2d}$$

$$\gamma_j = \sqrt{k_j^2 - \lambda^2}. \tag{2e}$$

King and Sandler [26], and Zhang and Pan [25] applied two approaches to solve the integral in (1c) for  $E_z^{(3)}$ . In the former paper, the integration part  $E_z^{(3)}$  was simplified as

$$E_z^{(3)} = -\frac{\omega\mu_0 k_0}{2} \sqrt{\frac{1}{\pi k_0 r_2}} \cdot \left( \frac{\rho}{r_2} \right) \varepsilon e^{ik_0 r_2} \cdot e^{-iP} F(P) \tag{3}$$

where

$$P = \frac{k_0 r_2}{2} \left( \frac{\varepsilon r_2 + z_r + z_s}{\rho} \right)^2 \tag{4a}$$

$$\varepsilon = \frac{k_0}{k_2} - ik_0 l \tag{4b}$$

$$F(P) = \frac{1}{2}(1+i) - \int_0^P \frac{e^{it}}{\sqrt{2\pi t}} dt. \tag{4c}$$

However, this modeling has a limited validation range as mentioned in [26], i.e., (3) must satisfy the following inequalities:

$$k_0^2 \ll k_1^2 \ll |k_2|^2 \tag{5a}$$

$$k_1^2 l^2 \ll 1 \quad \text{or} \quad k_1 l \leq 0.6. \tag{5b}$$

In the latter paper, if the second layer is perfectly conducting, the integration part  $E_z^{(3)}$  was simplified as [25]

$$E_z^{(3)} = E_z^{\text{sur}} + E_z^l \tag{6a}$$

$$E_z^{\text{sur}} = -\omega\mu_0 \sqrt{\frac{1}{2\pi\rho}} e^{i\frac{3\pi}{4}} \sum_i \frac{\gamma_1(\lambda_i^*) \tan(\gamma_1(\lambda_i^*)l) (\lambda_i^*)^{5/2}}{q'(\lambda_i^*) \gamma_0(\lambda_i^*)} \cdot e^{i\gamma_0(\lambda_i^*)(z_r+z_s) + i\lambda_i^* \rho} \tag{6b}$$

$$E_z^l = \frac{\omega k_0^2 \mu_0}{2k_1^2} \sqrt{\frac{1}{\pi k_0 \rho}} \sqrt{k_1^2 - k_0^2} \cdot \tan \sqrt{k_1^2 - k_0^2} l \cdot e^{i(k_0 r_2 + \pi/2)} \cdot e^{-iP^*} F(P^*) \tag{6c}$$

where

$$P^* = \frac{k_0 \rho}{2} \left( \frac{z_r + z_s}{\rho} - \frac{ik_0 \sqrt{k_1^2 - k_0^2}}{k_1^2} \tan \sqrt{k_1^2 - k_0^2} l \right)^2 \tag{7a}$$

$$\gamma_i^* = \sqrt{k_i^2 - k_0^2} \tag{7b}$$

and  $\lambda_i^*$  is the pole of (1c). The first term of (6) corresponds to the contribution of the surface wave denoted by  $E_z^{sur}$  and the second term represents the contribution of the lateral wave notated by  $E_z^l$ .

The formulas were extended to include an imperfectly conducting substrate in a later paper [8], where the trapped surface wave and the lateral wave were rewritten as

$$E_z^{sur} = - \frac{\omega \mu_0 e^{i\frac{\pi}{4}}}{2k_0^2} \sqrt{\frac{2}{\pi \rho}} \cdot \sum_i \frac{A(\lambda_i^*) \lambda_i^{*5/2}}{q'(\lambda_i^*) \gamma_0(\lambda_i^*)} e^{i\gamma_0(\lambda_i^*)(z_r + z_s) + i\lambda_i^* \rho} \tag{8a}$$

$$E_z^l = - \frac{\omega \mu_0}{2} \sqrt{\frac{k_0}{\pi \rho}} \varepsilon^* e^{ik_0 r_2} e^{-iP^*} F(P^*) \tag{8b}$$

where

$$P^* = \frac{k_0 \rho}{2} \left( \frac{\varepsilon^* \rho + z_r + z_s}{\rho} \right)^2 \tag{9a}$$

$$\varepsilon^* = \frac{\frac{\gamma_2^* k_0}{k_2^2} - i \frac{k_0 \gamma_1^*}{k_1^2} \tan \gamma_1^* l}{1 - i \frac{k_1^2 \gamma_2^*}{k_2^2 \gamma_1^2} \tan \gamma_1^* l} \tag{9b}$$

The trapped surface wave was proved to have a decay factor of  $\rho^{1/2}$  in the direction. It has been also shown that when the inequalities in (5) are satisfied, the lateral wave of  $E_z^l$  in (6c) is approximately the same as that in (3) [27].

For the spherical earth model, the earth is treated as a layered sphere. The center of the sphere is assumed to be at the origin of the spherical coordinate system (r,  $\theta$ ,  $\phi$ ). The radius of the earth is a. The dipole is located at a distance  $b=a+z_s$  from the center of the sphere. The radial distance of the observation point to the center of the sphere is  $r=a+z_r$ . The wave number in the air is  $k_0$ .

A direct relationship between the radiated field and current distribution can be expressed using the dyadic Green's function. For  $r \hat{U} b$ , the electric field in the outer space is expressed as [30]

$$\mathbf{E}(\mathbf{r}) = - \frac{\omega \mu_0 I_0}{4\pi b} \sum_{n=0}^{\infty} (2n+1) \cdot \begin{cases} [j_n(k_0 b) + \mathcal{B}_N^{11} h_n^{(1)}(k_0 b)] \mathbf{N}_{e0n}^{(1)}(k_0) \\ h_n^{(1)}(k_0 b) [\mathbf{N}_{e0n}(k_0) + \mathcal{B}_N^{11} \mathbf{N}_{e0n}^{(1)}(k_0)] \end{cases} \tag{10}$$

where  $N_{e0n}^{(1)}(k)$  and  $N_{e0n}$  denote the even vector eigenfunctions at  $m=0$  defined by [31]

$$\mathbf{N}_{e0n}^{(1)}(k) = \frac{n(n+1)}{kr} h_n^{(1)}(kr) P_n(\cos \theta) \hat{\mathbf{r}} + \frac{1}{kr} \frac{d[rh_n^{(1)}(kr)]}{dr} \frac{\partial P_n(\cos \theta)}{\partial \theta} \hat{\boldsymbol{\theta}} \tag{11a}$$

$$\mathbf{N}_{e0n}(k) = \frac{n(n+1)}{kr} j_n(kr) P_n(\cos \theta) \hat{\mathbf{r}} + \frac{1}{kr} \frac{d[rj_n(kr)]}{dr} \frac{\partial P_n(\cos \theta)}{\partial \theta} \hat{\boldsymbol{\theta}} \tag{11b}$$

with  $\mathcal{B}_N^{11}$  standing for the reflection coefficient.

Equation (10) represents the exact summation expressions for the electrical fields. The electric field radial component  $E_r$  is given by

$$E_r = E_0 e^{i\pi/4} \sqrt{\pi x} \sum_{s=1}^{\infty} \frac{1}{t_s - q^2} \frac{w_1(t_s - y_s)}{w_1(t_s)} \frac{w_1(t_s - y_r)}{w_1(t_s)} e^{it_s x} \tag{12}$$

where

$$E_0 = \frac{iI_0 \sqrt{\mu_0}}{2\pi \sqrt{\epsilon_0}} \frac{k_0 e^{ik_0 a \theta}}{a \sqrt{\theta \sin \theta}} \tag{13a}$$

$$y_s = \left(\frac{2}{k_0 a}\right)^{1/3} k_0 z_s \tag{13b}$$

$$y_r = \left(\frac{2}{k_0 a}\right)^{1/3} k_0 z_r \tag{13c}$$

$$x = \left(\frac{k_0 a}{a}\right)^{1/3} \theta \tag{13d}$$

$$q = \frac{k_0 \sqrt{k_1^2 - k_0^2}}{k_1^2} \left(\frac{k_0 a}{2}\right)^{1/3} \tan\left(\sqrt{k_1^2 - k_0^2} l\right) \tag{13e}$$

while  $\omega_1(t)$  denotes the Fock notation of the Airy function, and  $t_s$  represents the roots of the equation  $w_1'(t) - qw_1(t) = 0$ . (14)

The first term in (12) is the trapped surface wave, which is dominant. The residue series was extended to a spherical earth coated with an  $l$ -layered dielectric later by Li and Park [8]. It is stated that the coupling between the trapped surface wave and the lateral wave is not significant for the spherical earth model.

### 3. RESULTS AND DISCUSSION :

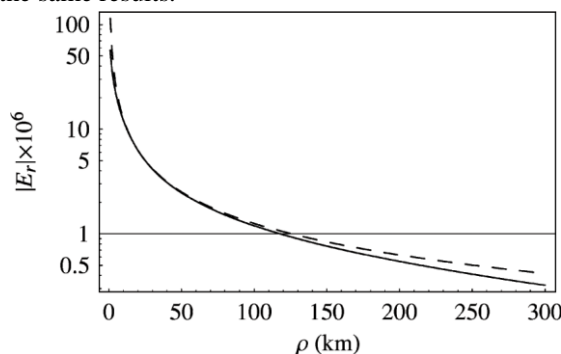
The residue series of spherical earth model is asymptotic as well—therefore, its accuracy needs to be investigated. In this subsection, the results obtained using the residue series are compared with those using the exact series expression. When the thickness of the dielectric layer is zero, the problem degenerates to a dipole radiating in the presence of a perfectly conducting plane or sphere. In this case, the image theory can be directly used to obtain the exact result for the planar model, i.e., the integral  $E_z^{(3)}$  of vanishes. For the spherical model, the image theory can be also used to approximate the field in the near field

$$\mathbf{E}_{\text{direct}}(\mathbf{r}) = -\frac{\omega \mu_0 I_0}{4\pi b} \frac{1}{k} \nabla \times \nabla \times \left[ \frac{e^{ikR}}{ikR} \mathbf{r} \right] \Big|_{b=(a+z_s)} \tag{15}$$

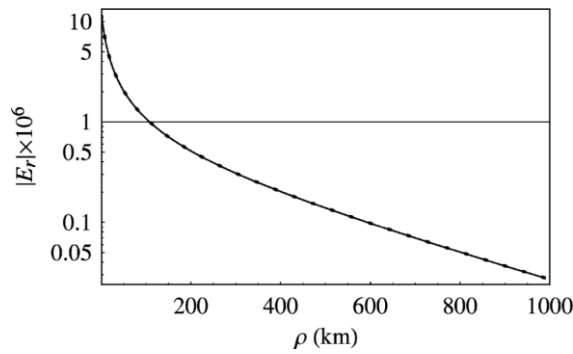
$$\mathbf{E}_{\text{image}}(\mathbf{r}) = -\frac{\omega \mu_0 I_0}{4\pi b} \frac{1}{k} \nabla \times \nabla \times \left[ \frac{e^{ikR}}{ikR} \mathbf{r} \right] \Big|_{b=(a-z_s)} \tag{16}$$

Fig. 1 shows the electric field of an electric dipole above the perfect conducting sphere. The results obtained using the approximate image in (15) and the residue series in spherical model are compared. The series of the formula in (12) converges slowly when the arc distance  $\rho \leq 50$  km. It is shown that within the range  $\rho \leq 100$  km, these two curves are almost the same. As the field point away from the source, the difference between these two methods are increased because of the curvature effects.

Fig. 2 shows the electric field in the spherical earth model which is assumed to be perfectly conducting. Results of the exact series summation of (10) are compared with those using the residue series approximation. For this case, the lateral wave vanishes and these two methods lead to exactly the same results.



**Fig. 1. Amplitudes of  $E_z$  varying with  $\rho$ , compared by approximate image (----) and residue series (—) with dielectric layer thickness  $l = 0$  m, at a frequency of  $f = 100$  kHz,  $z_s = 0$  m,  $z_r = 10$  m.**



**Fig. 2. Amplitudes of  $E_z$  varying with  $\rho$ , compared by exact series (—), and residue series (----) for PEC,  $z_s = 10\text{m}$ ,  $z_r = 500\text{m}$ , at a frequency of  $f = 100\text{ kHz}$ .**

It confirms the accuracy of the residue series for the perfect conducting spherical earth model.

Also we consider the situation in which the thickness of the dielectric layer is not zero. Figs. 2–4 show the  $E_r$  field for a coated spherical earth with a relative permittivity of  $\epsilon_r=1.1, 2.0$  and  $15$  for the dielectric layer, respectively. As shown in Fig. 3, when  $\epsilon_r$  of the dielectric layer is close to 1, the hybrid modes of the trapped surface wave and the lateral wave are not strong, so the curves obtained using these two formulas are still smooth and close to each other. The asymptotic residue formula and the exact series summation leads to almost the same result when the arc distance  $\rho \geq 50\text{km}$ .

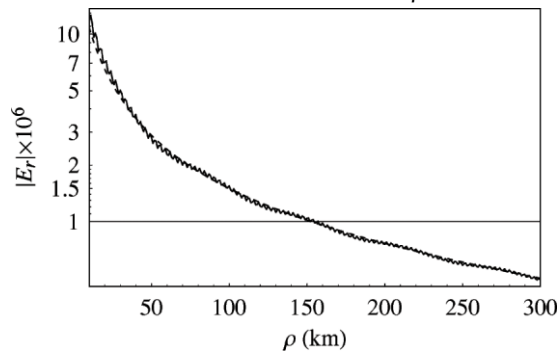


**Fig. 3. Amplitudes of  $E_z$  vary with  $\rho$ , compared by exact series (—), and residue approximation (---),  $z_s = 10\text{m}$ ,  $z_r = 500\text{m}$ ,  $\epsilon_r = 1:1, l = 100\text{m}$ , at frequency  $f = 100\text{ kHz}$ .**

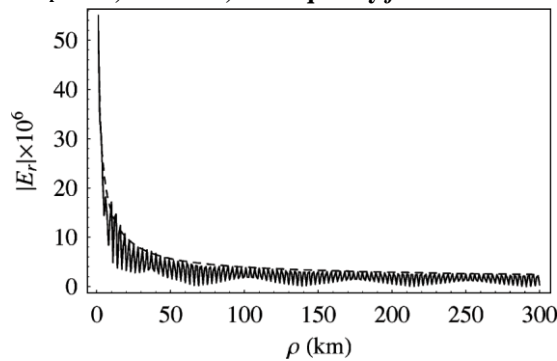


**Fig. 4. Amplitudes of  $E_z$  vary with  $\rho$ , compared by exact series (—), and residue approximation (---),  $z_s = 10\text{m}$ ,  $z_r = 500\text{m}$ ,  $\epsilon_r = 2.0, l = 100\text{m}$ , at frequency  $f = 100\text{ kHz}$ .**

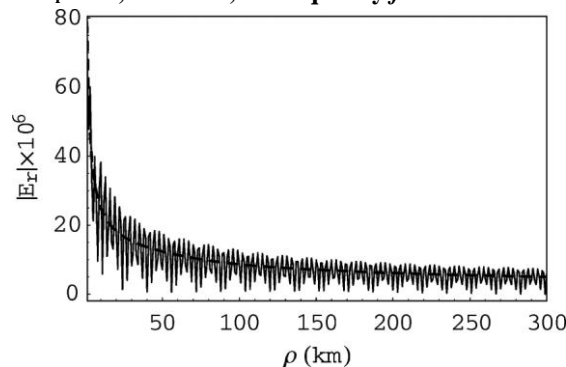


**Fig. 5. Amplitudes of  $E_z$  vary with  $\rho$ , compared by exact series (—), and residue approximation (---),  $z_s = 10\text{m}$ ,  $z_r = 500\text{m}$ ,  $\epsilon_r = 15, l = 100\text{m}$ , at frequency  $f = 100\text{ kHz}$ .**

In Fig. 4, where  $\epsilon_r=20$ , the curve obtained using the series summation begins showing small oscillations. In Fig. 5, where  $\epsilon_r=15$ , the oscillation of the curve obtained using the series summation becomes stronger with the increase of the permittivity of the dielectric layer while the curve obtained using the residue series still keeps to be smooth. Comparison among Figs. 1–4 shows that the curves obtained using the residue series are always very smooth while the oscillations in the curves obtained using the series summation exist due to the hybrid modes of the trapped surface wave and the lateral wave. Such surface waves can be considered to be the contribution of the multiply reflected guided waves among the dielectric slab, and the oscillation can be considered as the dielectric resonance between the upper and lower dielectric interfaces. It implies that the lateral wave travels along the interface, at the same time it is multiply reflected by the upper and lower dielectric surfaces when the dielectric constant is large.

#### 4. CONCLUSION :

The present analysis provides a very good picture on the validation studies of the classic problem defined and their solutions available in literature.

#### REFERENCES :

- [1] J. R. Johler and R. L. Lewis, "Extra low-frequency terrestrial radiowave field calculations with the zonal harmonic series," *J. Geophys. Res.*, vol. 74, no. 10, pp. 2459–2470, May 1969.
- [2] R. L. Lewis and J. R. Johler, "Correction of numerical results in 'ELF terrestrial radio wave field calculations with the zonal-harmonics series'," *Radio Sci.*, vol. 11, no. 2, pp. 75–81, Feb. 1976.
- [3] J. R. Johler, "Spherical wave theory for MF, LF, and VLF propagation," *Radio Sci.*, vol. 5, no. 12, pp. 1429–1443, Dec. 1970.
- [4] A. J. W. Sommerfeld, *Partial Differential Equations in Physics*. New York: Academic Press, 1949.
- [5] J. R. Wait, "Radiation from a vertical antenna over a curved stratified ground," *J. Res. National Bur. Standards*, vol. 56, no. 4, pp. 237–244, 1956.
- [6] V. A. Fock, *Electromagnetic Diffraction and Propagation Problems*. Oxford, U.K.: Pergamon, 1965.
- [7] W.-Y. Pan and H.-Q. Zhang, "Electromagnetic field of a vertical electric dipole on the spherical conductor covered with a dielectric layer," *Radio Sci.*, vol. 38, no. 3, 2003.
- [8] K. Li and S.-O. Park, "Electromagnetic field over the spherical earth coated with N-layered dielectric," *Radio Sci.*, vol. 39, 2004.
- [9] R. W. P. King and S. S. Sandler, "The electromagnetic field of a vertical electric dipole in the presence of a three-layered medium," *Radio Sci.*, vol. 29, pp. 97–113, Jan.–Feb. 1994.
- [10] R. W. P. King and S. S. Sandler, "The electromagnetic field of a vertical electric dipole over the earth or sea," *IEEE Trans. Antennas Propag.*, vol. 42, pp. 382–389, Mar. 1994.
- [11] A. Yokoyama, "Comments on 'the electromagnetic field of a vertical electric dipole over the earth or sea'," *IEEE Trans. Antennas Propag.*, vol. 43, pp. 541–542, May 1995.
- [12] J. R. Wait, "Remarks on the comments and reply on 'the electromagnetic field of a vertical electric dipole over the earth or sea'," *IEEE Trans. Antennas Propag.*, vol. 44, pp. 271–272, Feb. 1996.
- [13] J. R. Wait, "On the power absorbed by an electric dipole just above a conducting half space," in *Proc. IEEE Int. Antennas Propagat. Symp. Dig.*, 1997, pp. 240–243.
- [14] S. F. Mahmoud, "Remarks on 'the electromagnetic field of a vertical electric dipole over the earth or sea'," *IEEE Trans. Antennas Propag.*, vol. 47, pp. 1745–1746, Nov. 1999.
- [15] C. T. Tai and R. E. Collin, "Radiation of a hertzian dipole immersed in a dissipative medium," *IEEE Trans. Antennas Propag.*, vol. AP-48, no. 10, pp. 1501–1506, Oct. 2000.
- [16] S. R. Brueck, "Radiation from a dipole embedded in a dielectric slab," *IEEE Trans. Magn.*, vol. 6, no. 6, pp. 899–910, Nov./Dec. 2000.
- [17] R. E. Collin, "Some observations about the near zone electric field of a Hertzian dipole above a lossy earth," *IEEE Trans. Antennas Propag.*, vol. 52, pp. 3133–3137, Nov. 2004.
- [18] R. E. Collin, "Hertzian dipole radiating above a lossy earth or sea: Some early and late 20th century controversies," *IEEE Antennas Propag. Mag.*, vol. 46, no. 2, pp. 64–79, April 2004.
- [19] D. Dence and T. Tamir, "Radio loss of lateral waves in forest environments," *Radio Sci.*, vol. 4, p. 307, 1969.
- [20] T. Tamir, "Radio waves propagation along mixed paths in forest environments," *IEEE Trans. Antennas Propag.*, vol. AP-25, pp. 471–477, Jul. 1977.
- [21] A. Arutaki and J. Chiba, "Communication in three-layered conducting media with a vertical magnetic dipole," *IEEE Trans. Antennas Propag.*, vol. AP-28, pp. 551–556, Apr. 1980.
- [22] G. P. S. Cavalcante and A. J. Giardola, "Optimization of radio communication in media with three layers," *IEEE Trans. Antennas Propag.*, vol. AP-31, pp. 141–145, Jan. 1983.
- [23] L. W. Li, T. S. Yeo, P. S. Kooi, and M. S. Leong, "Radio wave propagation along mixed paths through a four-layered model of rain forest: An analytic approach," *IEEE Trans. Antennas Propag.*, vol. 46, no. 7, pp. 1098–1111, Jul. 1998.
- [24] L. W. Li, J. H. Koh, T. S. Yeo, M. S. Leong, and P. S. Kooi, "Radiowave propagation along mixed paths through a four-layered model of rain forest: An analytic approach," *IEEE Trans. Geosci. Remote Sensing*, vol. GRS-37, no. 4, pp. 1967–1979, Jul. 1999.

- [25] H.-Q. Zhang and W.-Y. Pan, "Electromagnetic field of a vertical electric dipole on a perfect conductor coated with a dielectric layer," *Radio Sci.*, vol. 37, no. 4, pp. 13-1–13-7, 2002.
- [26] R. W. P. King and S. S. Sandler, "The electromagnetic field of a vertical electric dipole in the presence of a three-layered region," *Radio Sci.*, vol. 29, no. 1, pp. 97–113, 1994.
- [27] H.-Q. Zhang, K. Li, and W.-Y. Pan, "The electromagnetic field of a vertical dipole on the dielectric-coated imperfect conductor," *J. Electromagn. Waves Applicat.*, vol. 10, no. 10, pp. 1305–1320, 2004.
- [28] K. Li, Y. Lu, and M. Li, "Approximate formulas for lateral electromagnetic pulses from a horizontal electric dipole on the surface of one-dimensionally anisotropic medium," *IEEE Trans. Antennas Propag.*, vol. 53, no. 3, pp. 933–937, 2005.
- [29] K. Li and Y. Lu, "Electromagnetic field generated by a horizontal electric dipole near the surface of a planar perfect conductor coated with a uniaxial layer," *IEEE Trans. Antennas Propag.*, vol. 53, no. 10, pp. 3191–3200, 2005.
- [30] C. T. Tai, *Dyadic Green's Functions in Electromagnetic Theory*, 2<sup>nd</sup> ed. Piscataway, NJ: IEEE Press, 1994.
- [31] J. A. Stratton, *Electromagnetic Theory*. New York: McGraw-Hill, 1941.